Time-sensitive reorganization of the somatosensory cortex poststroke depends on interaction between Hebbian and homeoplasticity: a simulation study

Amarpreet Singh Bains and Nicolas Schweighofer

J Neurophysiol 112:3240-3250, 2014. First published 1 October 2014; doi:10.1152/jn.00433.2013

J Neurophysiol 112: 3240–3250, 2014.
First published October 1, 2014; doi:10.1152/jn.00433.2013.

Time-sensitive reorganization of the somatosensory cortex poststroke depends on interaction between Hebbian and homeoplasticity: a simulation study

Amarpreet Singh Bains[1] and Nicolas Schweighofer[1,2,3]

[1]*Neuroscience Graduate Program, University of Southern California, Los Angeles, California;* [2]*Biokinesiology and Physical Therapy, University of Southern California, Los Angeles, California; and* [3]*M2H Laboratory, Euromov, University of Montpellier I, Montpellier, France*

Submitted 13 June 2013; accepted in final form 30 September 2014

Bains AS, Schweighofer N. Time-sensitive reorganization of the somatosensory cortex poststroke depends on interaction between Hebbian and homeoplasticity: a simulation study. *J Neurophysiol* 112: 3240–3250, 2014. First published October 1, 2014; doi:10.1152/jn.00433.2013.—Together with Hebbian plasticity, homeoplasticity presumably plays a significant, yet unclear, role in recovery postlesion. Here, we undertake a simulation study addressing the role of homeoplasticity and rehabilitation timing poststroke. We first hypothesize that homeoplasticity is essential for recovery and second that rehabilitation training delivered too early, before homeoplasticity has compensated for activity disturbances postlesion, is less effective for recovery than training delivered after a delay. We developed a neural network model of the sensory cortex driven by muscle spindle inputs arising from a six-muscle arm. All synapses underwent Hebbian plasticity, while homeoplasticity adjusted cell excitability to maintain a desired firing distribution. After initial training, the network was lesioned, leading to areas of hyper- and hypoactivity due to the loss of lateral synaptic connections. The network was then retrained through rehabilitative arm movements. We found that network recovery was unsuccessful in the absence of homeoplasticity, as measured by reestablishment of lesion-affected inputs. We also found that a delay preceding rehabilitation led to faster network recovery during the rehabilitation training than no delay. Our simulation results thus suggest that homeoplastic restoration of prelesion activity patterns is essential to functional network recovery via Hebbian plasticity.

stroke rehabilitation; computational model; Hebbian plasticity; homeoplasticity; rehabilitation timing

IT IS WIDELY APPRECIATED THAT motor rehabilitation given after a prolonged delay poststroke is less effective than after a short delay (Biernaskie et al. 2004; Horn et al. 2005; Maulden et al. 2005; Salter et al. 2006; Wolf et al. 2006, 2010), presumably because of the ending of the critical period for plasticity that characterizes the semiacute poststroke phase (Cramer and Chopp 2000; Murphy and Corbett 2009). However, rehabilitation given too early may also lead to subpar outcomes (Bland et al. 2000; Dromerick et al. 2009; Kozlowski et al. 1996; Risedal et al. 1999). For instance, in rodents, rehabilitative training that started 24 h after cortical infarct led to worse recovery than training that started 7 days after infarct, although recovery was still better than without training (Risedal et al. 1999). In humans, intense motor rehabilitation within 2 wk poststroke led to poorer outcomes than less-intense therapy during the same period (Dromerick et al. 2009).

Address for reprint requests and other correspondence: A. S. Bains, Neuroscience Graduate Program, Univ. of Southern California, Los Angeles, CA (e-mail: abains05@gmail.com).

The mechanisms underlying the subpar effects of too early rehabilitation are not well understood. Abnormal cortical patterns of excitation and inhibition occur both near (Clarkson et al. 2010; Liepert et al. 2000; Mittmann et al. 1998; Qu et al. 1998; Schiene et al. 1996) and far from the lesion (Buchkremer-Ratzmann and Witte 1997; Butefisch et al. 2003). Such abnormal excitability and resulting abnormal activity patterns are in part due to the loss of efferent connections from lesioned cells to local and distant areas (Buchkremer-Ratzmann and Witte 1997; Sober et al. 1997). Locally, pyramidal cells send lateral projections up to 2 mm away (Boucsein et al. 2011) with net excitatory effects to nearby cells and net inhibitory effects to more distant cells, via connections to local GABAergic neurons (Derdikman et al. 2003). Computer simulation studies using such "Mexican hat" connectivity patterns (Sirosh and Miikkulainen 1997; Stevens et al. 2013; Sullivan and de Sa 2006; Wilson et al. 2010) have supported the experimental findings that lesions yield complex changes in activity, with zones of abnormally low and high excitability (Goodall et al. 1997; Sober et al. 1997). Abnormal hyperexcitability, if exacerbated by activity due to early and intense use of the affected limb, can cause cell death and lesion enlargement (Risedal et al. 1999), presumably via abnormally high levels of NMDA activity (Humm et al. 1999; Risedal et al. 1999). In surviving cells, hyperexcitability enhances Hebbian plasticity-like long-term potentiation (LTP) perilesionally (Hagemann et al. 1998). Such increased plasticity may be beneficial to recovery (Hagemann et al. 1998; Murphy and Corbett 2009), because it can help in the strengthening and reemergence of remaining weak afferent synapses from stroke-affected inputs (Jones 2000; Sanes and Donoghue 2000; Sigler et al. 2009; Winship and Murphy 2009). However, increased LTP may also lead to maladaptive plasticity and poor cortical reorganization if existing inputs are further strengthened at the expense of the reemergence of weak afferent synapses.

In addition to Hebbian plasticity-like LTP, homeoplasticity has been proposed to play a significant role postlesion (Murphy and Corbett 2009; Nahmani and Turrigiano 2014). Homeoplasticity, which is ubiquitous in the brain, acts to maintain desired firing rates and patterns (Desai et al. 1999; LeMasson et al. 1993; Turrigiano 2011). In response to abnormally low or high activity after lesion, homeoplasticity may thus enhance or decrease excitability, respectively, to restore prelesion firing levels (Murphy and Corbett 2009).

Experimentally, it is difficult to study the interacting effects of homeoplasticity, LTP, and enhanced inputs due to rehabilitative training on cortical reorganization and recovery postle-

sion (Murphy and Corbett 2009; Nahmani and Turrigiano 2014). In addition, rehabilitative training will affect the network differently at different times poststroke depending on the level of "spontaneous recovery" achieved before training. Here, we aim at better understanding these interactions in computer simulations to guide future experimental work and, eventually, clinical practice regarding the optimal timing of rehabilitation. We make the following two hypotheses. First, homeoplasticity, together with Hebbian plasticity, enhances recovery and prevents maladaptive cortical reorganization. Second, rehabilitation training delivered too early, before homeoplasticity has compensated for activity disturbances postlesion, is less effective for network recovery than training delivered after a delay.

To test these hypotheses, we developed a simplified somatosensory cortical network of neurons that received simulated arm muscle spindle inputs and lateral connections via Mexican hat-like connectivity. All synapses were modifiable via Hebbian plasticity; cell activity was adjusted via homeoplasticity. After initial cortical organization in response to arm reaching movements, the network was partly lesioned to simulate a stroke. We first tested the specific contribution of homeoplasticity to network reorganization and then tested the effect of rehabilitation timing.

MATERIALS AND METHODS

Arm and Muscle Spindle Simulations

We simulated a planar two-joint kinematic human arm model with shoulder and elbow joints. Each joint was spanned by an extensor and flexor muscle pair, as well as a biarticular pair (Fig. 1) (Katayama and Kawato 1993). These muscles are abbreviated as Sh-Fl and Sh-Ex for the shoulder, El-Fl and El-Ex for the elbow, and Bi-Fl and Bi-Ex for the biarticular pair, with Fl and Ex denoting flexor and extensor. Each muscle was passively stretched and contracted during reaching movements and gave rise to two spindle activities, one based on muscle length (similar to a group II fiber) and the other on the sum of length and stretch velocity (similar to a group Ia fiber).

Planar point-to-point movements were generated via a minimum jerk model (Flash and Hogan 1985). Inverse kinematics generated shoulder and elbow angles. Movement endpoints were randomly selected with the constraint that changes in shoulder and elbow angles during each movement were required to be less than $\pi/4$ and $\pi/3$ radians, respectively. The time *MT* allowed for each movement was based on a modified Fitts's law $MT = \log_2(a + distance)$ (MacKenzie 1989), where *distance* is the Cartesian distance between consecutive endpoints and $a = 1.3$. The stretch lengths and velocities of each muscle were normalized to between 0 and 1 to keep all spindle activity ranges equal. Time step length was 0.01 s.

Cortical Network Simulations

A 400-cell (20×20) network arranged in a doughnut-shaped grid received the 12 spindle inputs. This represented a small patch of primary sensory cortex. Before training, initial connection weights from spindles to cortical cells were all-to-all, chosen randomly from the range [0,1] before being normalized to sum to 1 for each cell. Cells were laterally connected to each other with Mexican hat connectivity (Kohonen 1982; Lytton et al. 1999; Sirosh and Miikkulainen 1997; Sober et al. 1997; Stevens et al. 2013; Sullivan and de Sa 2006; Wilson et al. 2010).The lateral weight L_{ij} from cell j to i was defined as:

$$L_{ij} = \frac{A_e}{\sigma_e\sqrt{2\pi}} e^{-\frac{d^2}{2\sigma_e^2}} - \frac{A_i}{\sigma_i\sqrt{2\pi}} e^{-\frac{d^2}{2\sigma_i^2}}$$

where d is the grid distance between the cells, and other parameter values are given in Table 1.

Positive and negative lateral input weights to each cell were normalized to sum to 9 and -9, respectively. Such bias in the strength of lateral vs. afferent input has been found in cortical pyramidal cells

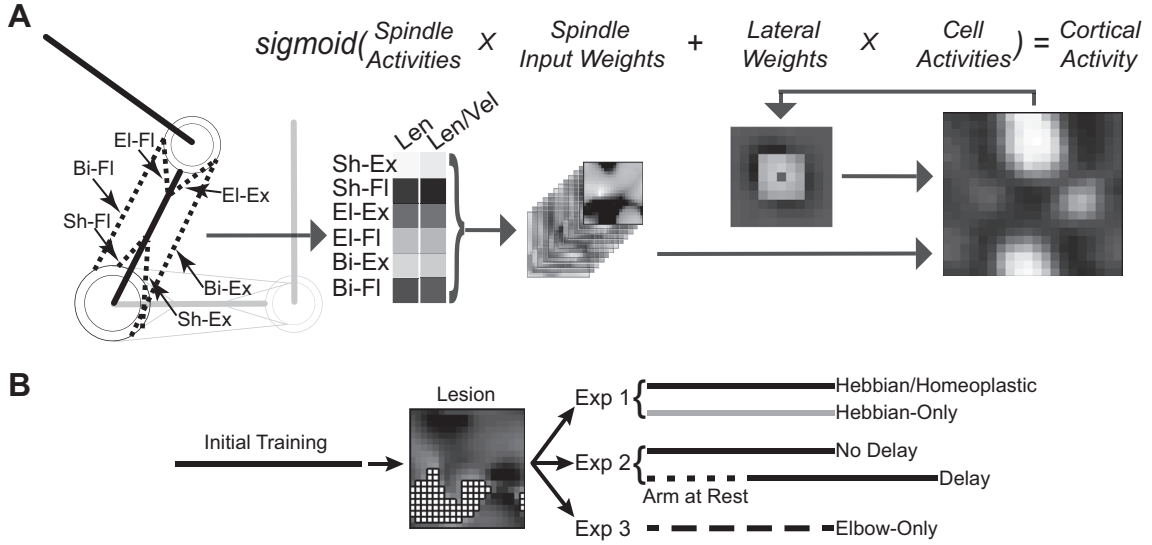

Fig. 1. Model and simulated experiments. *A*: effects of arm movement on cortical activity. *Left* to *right*: simulated 2-joint, 6-muscle arm during movement (background shows arm in home position for reference). Black dashed lines are muscles and include shoulder flexor and extensor (Sh-Fl and Sh-Ex), elbow flexor and extensor (El-Fl and El-Ex), and biarticular flexor and extensor (Bi-Fl and Bi-Ex). The 6-by-2 pixel grid shows corresponding activity in Length-Only and Length/Velocity spindles for each muscle. As input to cortical cells, spindle activities were multiplied by input weights (shown as stack of weight maps) to cells. Each map pixel shows weight from 1 spindle to 1 cortical cell; different maps represent weights from different spindles. Each cell also received weighted activity from neighboring cells as input, with weights in a Mexican hat pattern (*plot second* from *right* shows example of lateral weights from nearest 120 neighbors to cell at center of grid). Summed input from spindles and neighbors ("membrane potential") was passed through a sigmoid function to generate each cortical cell activity, shown on *far right* (each pixel is activity of 1 cell). *B*: schematic demonstrating time course of initial network training period, lesion, and rehabilitation training in *experiments 1* and *2*, as well as postlesion Elbow-Only training in *experiment 3*.

Table 1. *Values of all the parameters used in the model*

Model Parameters	Values
Mexican hat parameters	
A_e	10
σ_e	1.5
A_i	5
σ_i	2.5
Plasticity parameters	
η_{hebb}	0.03
η_{hom}	0.001
μ_{hom}	0.3
Spindle input weight normalization constant	1
Positive lateral weight normalization constant	9
Negative lateral weight normalization constant	−9
Cell dynamics parameters	
Δt	0.01
τ	0.01

(Boucsein et al. 2011; Stepanyants et al. 2009). Normalization constants and difference-of-Gaussian parameters were heuristically chosen based on two criteria. *1*) Formation of contiguous cell neighborhoods (as defined by strong input weights from the same subset of spindles) following initial training. *2*) Large activity disturbances throughout the network following lesions targeting given neighborhoods (see *Lesioning*).

Each cell was modeled as a simple leaky integrator neuron (Arbib 1995). The change in "membrane voltage" of cell i at time t was given by:

$$\tau\frac{\Delta x_{t,i}}{\Delta t} = -x_{t,i} + \sum_{k=1}^{12} S_{ik}f_{t,k} + \sum_{j=1}^{400} L_{ij}y_{t,j},\ i \neq j \qquad (1)$$

where $x_{t,i}$ is the voltage for cell i at time t, $y_{t,j}$ is the activity for cell j ($i \neq j$) at time t, L_{ij} is the lateral connection weight from cell j to i, S_{ik} is the synaptic connection weight from spindle k to cell i, $f_{t,k}$ is the activity of spindle k at time t, τ is the cell excitation constant, and Δt is the time step length in seconds. The voltage $x_{t,i}$ was then passed through a sigmoidal response curve to give a final cell activity, or "firing rate," $y_{t,i}$:

$$y_{t,i} = \frac{1}{1 + e^{-(a_i x_{t,i} + b_i)}}, \qquad (2)$$

where both the slope a_i and the offset b_i are adjusted via homeoplastic mechanisms in *Eqs. 4* and *5* below.

Hebbian Plasticity and Homeoplasticity

At each time step, afferent and lateral (positive and negative) weights were modified via Hebbian-type learning as follows:

$$w_{t+\Delta t} = w_t + \eta_{hebb}\, y_{pre,t}\, x_{post,t} \qquad (3)$$

where $y_{pre,t}$ and $x_{post,t}$ are the presynaptic cell or spindle activity and postsynaptic cell voltage, respectively, at time t, and η_{hebb} is the Hebbian learning rate (Castillo et al. 2011; Citri and Malenka 2008; Foldiak 1990; Madison et al. 1991). Only the magnitude, not the sign, of the weights could change. Weights were renormalized after each update to prevent runaway weight values. The normalization created competition between weights, whereby one weight to a cell could not increase without decreasing the contributions of other weights. Such competitive Hebbian learning is known to lead to regular map formation in models of sensory cortex (Kohonen 1982; Linsker 1989; Malsburg 1973; Wilson et al. 2010).

To model homeoplasticity, the slope and the offset of each cell's response curve (*Eq. 2*) were modified at each time step with the goal of maintaining an exponential firing rate distribution with a desired mean, according to Butko and Triesch (2006) and Triesch (2005). For cell i, the changes of sigmoidal parameters a_i and b_i in *Eq. 2* are given by:

$$\Delta a_i = \eta_{hom}\left[\frac{1}{a_i} + x_i - \left(2 + \frac{1}{\mu_{hom}}\right)x_i y_i + \frac{1}{\mu_{hom}}x_i y_i^2\right] \qquad (4)$$

$$\Delta b_i = \eta_{hom}\left[1 - \left(2 + \frac{1}{\mu_{hom}}\right)y_i + \frac{1}{\mu_{hom}}y_i^2\right] \qquad (5)$$

where η_{hom} is a learning rate and with μ_{hom} the mean of the exponential distribution (see Table 1 for parameter values and initial values).

Initial Network Training

Using spindle activities generated by 400 simulated arm movements (a total training length of 24,693 time steps) as inputs, we trained 10 different networks with a different random number generator seed for each network. The distribution of MT during these 400 movements was 0.62 ± 13 s (mean ± SD).

Lesioning

After initial training, the 10 cortical networks were lesioned by removing all cells with an input weight from the shoulder flexor length/velocity spindle (abbreviated as the Sh-Fl Len/Vel spindle) >0.1. Lesioning a specific spindle is similar to experimental approaches targeting the somatotopic representations of specific limbs or limb segments (see for instance, Brown et al. 2009; Kleim et al. 2003; Nudo et al. 1996).

Rehabilitation Training

After lesioning, the poststroke rehabilitation phase consisted of the same sequence of arm movements as in the training phase under each of the following conditions.

Simulated experiment 1: Hebbian/Homeoplastic vs. Hebbian-only rehabilitation. To test the importance of homeoplasticity in network recovery, rehabilitation training with both Hebbian and homeoplastic mechanisms active was compared with training with only the Hebbian mechanism active (η_{hom} was set to 0).

Simulated experiment 2: Delay vs. No Delay rehabilitation. To test the effect of rehabilitation timing, training was given either immediately after lesion (No Delay condition) or after a delay period (Delay condition). During the delay, only spindle activity stemming from the home position lengths of the six muscles was provided as input to the network. These activities were between 0.4 and 0.6 for all 12 spindles, in the middle of the possible [0,1] range of activity. For the main results, the delay length was equivalent to 50% of the 24,693 time steps of initial training, or 12,346 time steps. To link with *experiment 1*, the delay period was also simulated with only Hebbian plasticity present. We also explored the effect of variable delays in a parameter sensitivity analysis (see below).

Simulated experiment 3: Elbow-Only training after lesion. After infarct affecting the forelimb representation in monkey sensorimotor cortex, the absence of forced forelimb use and retraining prevents recovery of the forelimb cortical representation (Nudo and Milliken 1996; Nudo et al. 1996). To qualitatively compare the reorganization of our networks to these results, we administered a type of degraded postlesion training in which spindle activities from the shoulder flexors and extensors were held at the values generated in the home arm position; other spindle activities were as during normal rehabilitative training above.

Outcome Measures

Mean cortical cell activities. Mean cell activities were calculated by averaging the activity of each cell in the network over a set number of simulation time steps (precise numbers noted in RESULTS for different situations). To quantify abnormal activity, the mean cell activities taken

across all time steps in initial training were subtracted from the mean cell activities during the period of interest (e.g., during rehabilitation) on a cell-by-cell basis. The mean ± SD of the absolute value of this change in mean activity was then calculated across cells and across simulations arising from different random number seeds.

Spindle input weight map and proportion changes. We measured the degree of recovery by comparing the input maps before lesion and at different time points after lesion. Specifically, for each spindle, 20 × 20 input weight maps were created by plotting the strength of input from this spindle to each of the 400 cells. Comparisons between post- and prelesion maps were quantified using the weight proportion change for each spindle, calculated as follows. The sum of input weight to all surviving cortical cells for a given spindle was divided by the sum of input weights to all surviving cells from all 12 spindles (there were 400 surviving cells prelesion, but this was reduced after lesion). This proportion (expressed as a percentage) was then compared at different times postlesion to the spindle's average proportion prelesion (across the final 6,000 time steps of training, i.e., after map organization had converged). Recovery had occurred when the difference in proportion from prelesion was no longer significantly different from 0% for the lesion-targeted Sh-Fl Len/Vel spindle. Significance was defined at the $P = 0.05$ level using the Wilcoxon signed rank test, using the 10 network simulations as the sample. Weight proportion change thus allowed an intuitive link with experimental work, where the reduction or expansion of somatotopic representations of different limb segments is one of the outcomes of interest after postinfarct rehabilitation or skill learning (Kleim et al. 1998; Nudo et al. 1996; Plautz et al. 2000).

Cell allegiance changes. At any single time point, one spindle has the largest input weight to a given cortical cell. Because of competitive Hebbian plasticity, this spindle can eventually have a lower weight to the cell than one of the other 11 spindles. If this happens, it is termed an "allegiance change," since the cell changes the spindle with which it has the strongest allegiance. Allegiance changes were used to quantify the degree of synaptic plasticity occurring postlesion, since such plasticity was necessary for reorganization of cortical inputs. To compare the Hebbian/Homeoplastic and Hebbian-Only conditions, the number of allegiance changes per cell was computed over the entire rehabilitation training.

Parameter sensitivity analyses. To check that the simulation results were not based on precisely tuned parameters alone, we ran rehabilitation simulations with different delay lengths (0, 12.5, 25, 37.5, 50, 62.5, and 75%), Hebbian learning rates (0, 0.0003, 0.003, 0.03, and 0.3), and homeoplastic learning rates (0, 0.0001, 0.001, 0.01, and 0.1). For each parameter, we ran six simulations with different random number seeds and computed lesion-targeted Sh-Fl Len/Vel input weight proportion change to quantify the degree of recovery.

RESULTS

Initial Network Training

As expected with competitive Hebbian learning, the initial random distribution of input weights from a given spindle to the cortical network (representing a small patch of primary sensory cortex) became organized into well-defined neighborhoods of relatively high input strength (Fig. 2*A*). During the final 6,000 time steps of training, each spindle contributed between 7.8 and 8.8% (averaged across time steps and simulations) of the total cortical input weight. The similar contributions reflected the similar percentage of total input activity accounted for by each spindle over time, averaging between 8.2 and 8.5%. Note that because of correlations or anticorrelations in spindle activities (see APPENDIX), spindle pairs had overlapping and nonoverlapping weight map distributions, respectively. Because there was very large overlap in the map

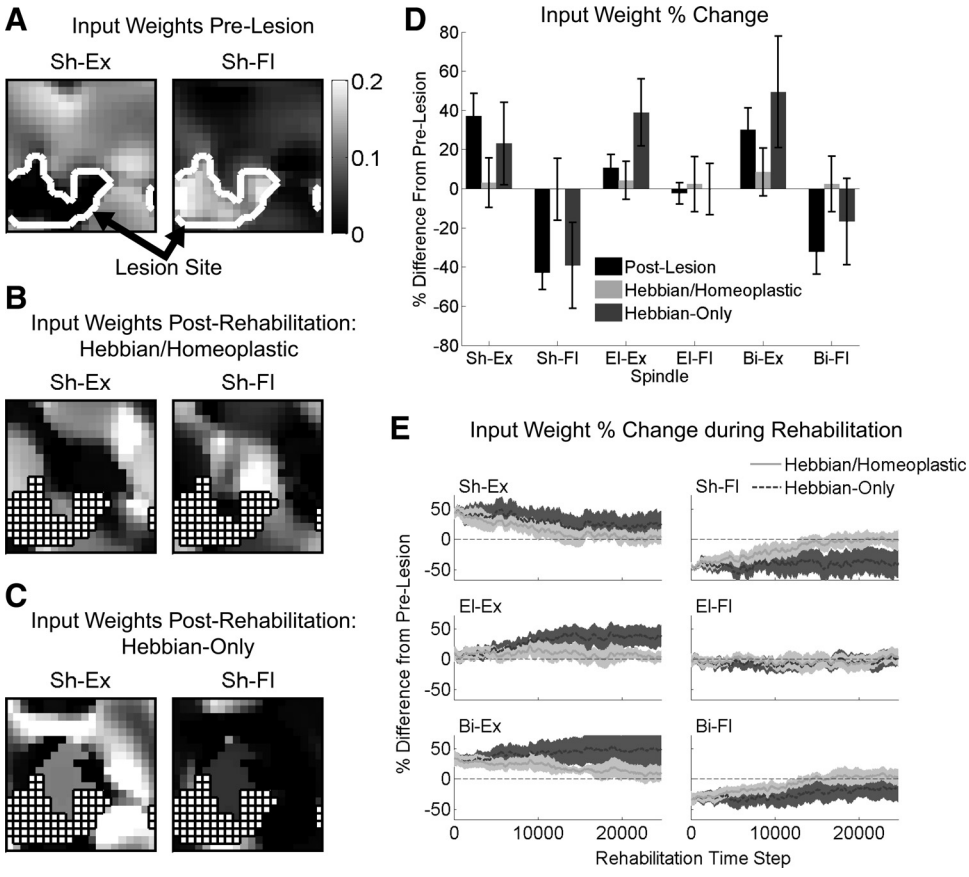

Fig. 2. Effects of initial training, lesion, and rehabilitation on spindle weight input representations in *experiment 1*. *A*: input weight maps from shoulder muscle spindles to cortical cells at end of training. Brightness denotes strength of input weight. White border denotes area to be lesioned. *B*: input weight maps for shoulder spindles after Hebbian/Homeoplastic condition. Here and in *C*, hatched region denotes lesion. *C*: input weight maps for shoulder spindles after Hebbian-Only condition. Note the lesion-targeted Sh-Fl spindle shows diminished areas of representation compared with the Hebbian/Homeoplastic condition in *B*. *D*: percent difference from prelesion of each spindle's input weight proportion after lesion and at the end of rehabilitation. Error bars represent mean ± SD. 0% Denotes recovery of the prelesion proportion. *E*: percent difference from prelesion of each spindle's input weight proportion during rehabilitation. Note for the lesion-targeted Sh-Fl spindle, recovery only occurs in the Hebbian/Homeoplastic condition. Shaded error represents mean ± SD.

distributions of length/velocity and length-only spindles arising from the same muscle, only results for the length/velocity spindles are shown hereafter.

Effects of Targeted Lesion

To simulate a stroke lesion, all cells with input weights from the Sh-Fl length/velocity spindle >0.1 were removed from the network. This lesion criterion resulted in 31 ± 7.0% (mean ± SD) of cells being lesioned and removed from each network. The postlesion input weight proportion for the targeted Sh-Fl spindle was reduced by 43 ± 8.7% across simulation seeds (Fig. 2*D*). The Bi-Fl spindle also experienced a weight proportion decrease of 32 ± 11% due to its significant cortical representation overlap with the Sh-Fl spindle.

Lesions caused large disturbances in mean cell activities of surviving cells by removing a large fraction of lateral connections. Figure 3, *A* and *B*, demonstrates this for one network by showing mean network activity after initial training either pre- or postlesion (computed over the same 3,000 time steps of spindle activity). The lesion caused persistent hyperactivity in local areas of the network, which then inhibited surrounding areas, causing them to exhibit low activity.

Experiment 1: Essential Role of Homeoplasticity in Recovery

We next addressed our first hypothesis, that homeoplasticity enhanced recovery of spindle input weight representations in the network after lesion. Figure 2 shows that the lesion-targeted Sh-Fl spindle recovered its prelesion input weight proportion by the end of the rehabilitation training in the Hebbian/Homeoplastic rehabilitation (recovery defined in MATERIALS AND METHODS using the Wilcoxon signed rank test). In contrast, in the Hebbian-Only rehabilitation, there was no recovery: the postlesion Sh-Fl proportion remained significantly different from prelesion. Similarly, the other spindles recovered in the Hebbian/Homeoplastic condition but did not recover their prelesion proportions in the Hebbian-Only condition.

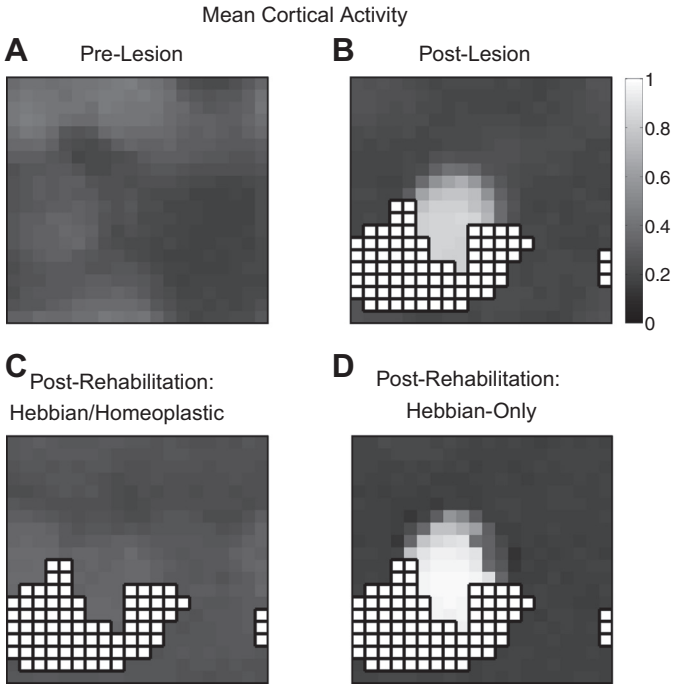

Fig. 3. Mean cortical cell activity before and after lesion and rehabilitation. *A*: mean activity of cortical cells (each represented as a single pixel) when network is presented with 3,000 time steps of arm movement after the end of the training dose in the absence of a lesion. Brightness denotes activity level. *B*: mean activity of cortical cells after lesion in response to the same 3,000 time steps of arm movement after training. Here and in *C* and *D*, hatched region denotes lesion. *C*: mean cortical cell activity over rehabilitation dose during Hebbian/Homeoplastic condition. *D*: mean cortical cell activity over rehabilitation dose during Hebbian-Only condition.

The different recovery patterns seen in the Hebbian/Homeoplastic and Hebbian-Only conditions were driven by greatly different cell activity patterns during rehabilitation training. Figure 3, *C* and *D*, shows the mean cell activities during rehabilitation for both Hebbian-Only and Hebbian/Homeoplastic rehabilitation. Compared with the Hebbian/Homeoplastic condition, activity remained persistently high or low in localized areas in the Hebbian-Only condition, similar to the activity patterns seen immediately after lesion in Fig. 3*B*. Under the Hebbian-Only condition, the absolute value of the change in mean cell activities compared with initial training was 0.13 ± 0.14 (mean ± SD across simulations and surviving cells). Such large changes in mean contrasted to the small activity changes in the Hebbian/Homeoplastic condition, which showed an absolute value of 0.041 ± 0.029 ($P <$ 1e-172, using the Wilcoxon rank sum test to compare conditions; significantly difference between conditions).

The difference in cell activities under each condition was driven by the presence or absence of homeoplasticity. Importantly, the direct effect of homeoplasticity on cell activity was the first link in a chain whereby homeoplasticity ultimately affected Hebbian plasticity and hence network reorganization.

The next link connected activity levels with cell membrane potentials. Although the activity of any cell in isolation had no way of affecting the cell's own membrane potential, in the laterally connected network the activity could affect the membrane potentials of other cells. Thus by altering the activities of the cells, homeoplasticity also indirectly changed the distribution of membrane potentials in the network. This effect is seen in the different distributions of mean cell membrane potentials (mean taken over rehabilitation training) under the Hebbian/Homeoplastic and Hebbian-Only conditions (Fig. 4*A*).

In the final link, homeoplasticity's effect on membrane potentials allowed it to affect Hebbian weight plasticity (see *Eq. 3*) and hence network reorganization, quantified here by cell allegiance changes during rehabilitation. Figure 4*B* demonstrates the close relationship between membrane potential and allegiance changes. By affecting the membrane potentials of the cells, homeoplasticity affected Hebbian spindle input weight changes through the membrane potential term in the Hebbian rule (*Eq. 3*). In particular, cells in the Hebbian-Only condition with near-zero mean membrane potential did not exhibit the allegiance changes needed for recovery: under the Hebbian-Only condition, 34.9 ± 17.1% (mean ± SD across simulations) of cells had few (less than 10) allegiance changes during rehabilitation training, vs. only 1.0 ± 0.91% for the Hebbian/Homeoplastic condition. The cells with <10 allegiance changes in the Hebbian-Only condition are shown in Figure 4*C*, along with the number of allegiance changes in the same cells under the Hebbian/Homeoplastic condition. This demonstrates that the same cells that contributed little to reorganization in the Hebbian-Only condition were not similarly impotent in the Hebbian/Homeoplastic condition.

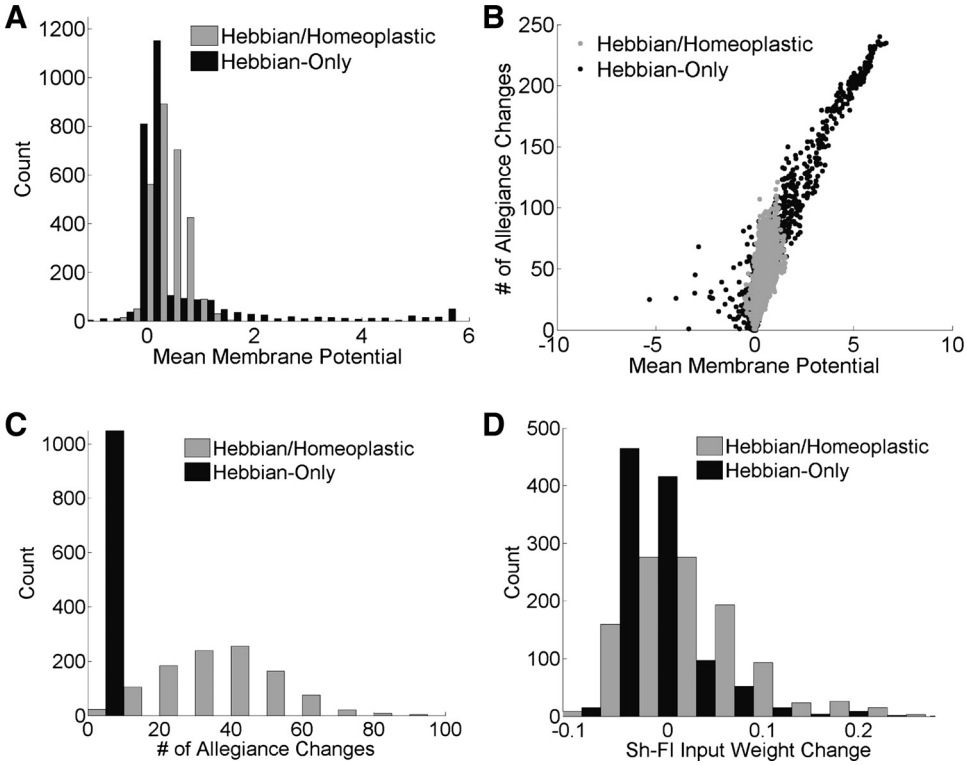

Fig. 4. Relationship between mean cell membrane potentials and spindle input weight plasticity in the Hebbian/Homeoplastic and Hebbian-Only conditions. *A*: distributions of mean cell membrane potentials during rehabilitation under both conditions. Note the clustering around zero in the Hebbian-Only condition. *B*: relationship between mean membrane potential and the number of cell allegiance changes (defined as a change in the spindle with the highest input weight to a cell). The 2 values are highly correlated because membrane potential drives synaptic plasticity according to the Hebbian rule (*Eq. 3*), which in turn leads to allegiance changes. *C*: only cells with few (<10) allegiance changes in the Hebbian-Only condition are shown. The same cells with <10 allegiance changes in the Hebbian-Only condition exhibit many more changes under the Hebbian/Homeoplastic condition. *D*: connection between allegiance changes and increase in weight (i.e., recovery) from the lesion-targeted Sh-Fl spindle. For the same cells as in *C*, the histogram shows changes in Sh-Fl spindle weight from the beginning to end of rehabilitation. Note the shift towards higher positive values in the Hebbian/Homeoplastic condition.

Importantly, for the cells with <10 allegiance changes in the Hebbian-Only condition, the input weight from the lesion-targeted Sh-Fl spindle decreased by −0.016 ± 0.046 (mean ± SD). In contrast, in the Hebbian/Homeoplastic condition, input weight from the lesion-targeted Sh-Fl spindle increased by 0.031 ± 0.079 (Fig. 4*D*). This illustrates the connection between reorganization and recovery: cells with few allegiance changes experienced little gain in Sh-Fl input strength, so the chain mechanistically linking homeoplasticity to reorganization and increased allegiance changes also linked it to recovery.

Experiment 2: Effect of Delayed Rehabilitation Training

We found our second hypothesis, that rehabilitation delivered immediately after lesion (No Delay condition) is less effective than one delivered after a delay (Delay condition; see Fig. 1*B*), was true due to the following mechanism. Driven by similar activity from all spindles during the delay period, many cells decreased their input weights from previously strongly connected spindles and increased weights from previously weakly connected spindles, making weights more similar (or "flattened") across spindles. For each cell, this change was gauged by calculating the standard deviation of input weights across all 12 spindles before and after the delay, since more flattened weights would give rise to a smaller standard deviation. Indeed, the input weight standard deviation per cell fell from 0.053 ± 0.017 (mean ± SD) immediately postlesion to 0.026 ± 0.025 after the delay. In particular, since the lesion left alive only cells with weak weights from the Sh-Fl spindle, the flattening of input weights increased weight from this spindle on average. Immediately postlesion, the average input weight value from the Sh-Fl spindle was 0.048 ± 0.024 per cell (mean ± SD across simulations and surviving cells), while it increased to 0.064 ± 0.017 after the delay (see Fig. 5, *A* and *B*).

Thus rehabilitation after delay began with similar weight values from all spindles. This allowed the Sh-Fl weights to compete more effectively with spindles that would have had much higher weights before the delay, thereby speeding recovery (Fig. 5*C*). Although recovery of weight proportions for lesion-targeted Sh-Fl spindle occurred in both conditions, recovery occurred after 13,032 time steps of rehabilitation in the No Delay condition but only after 4,550 time steps in the Delay condition, a 65% faster recovery (Wilcoxon signed rank test was used to measure recovery, as explained in MATERIALS AND METHODS).

The beneficial effect of delay depended on homeoplasticity: in a simulation of Hebbian-Only plasticity during the delay, input weights did not flatten to the same degree during the delay. In particular, the average Sh-Fl weight remained at 0.052 ± 0.024 (mean ± SD across simulations and surviving cells) after delay without homeoplasticity, little-changed from immediately postlesion compared with the Sh-Fl weights after the delay with homeoplasticity.

Experiment 3: Effects of Elbow-Only Training after Lesion

During Elbow-Only training postlesion, the input weight proportion from the lesion-targeted Sh-Fl spindle showed no recovery of representation across all simulation seeds (see Fig. 6). The spindle's input weight proportion immediately after lesion was reduced by 44.8 ± 4.7% (mean ± SD) compared with prelesion, and after postlesion training it was still reduced by 33.3 ± 9.1%. There was also loss of representation of the shoulder extensor spindle Sh-Ex due to its inactivity during the Elbow-Only training. Immediately after lesion, it had increased its weight proportion by 45.7 ± 10.1% compared with prelesion, but by the end of training this had become a decrease of 10.5 ± 5.9%.

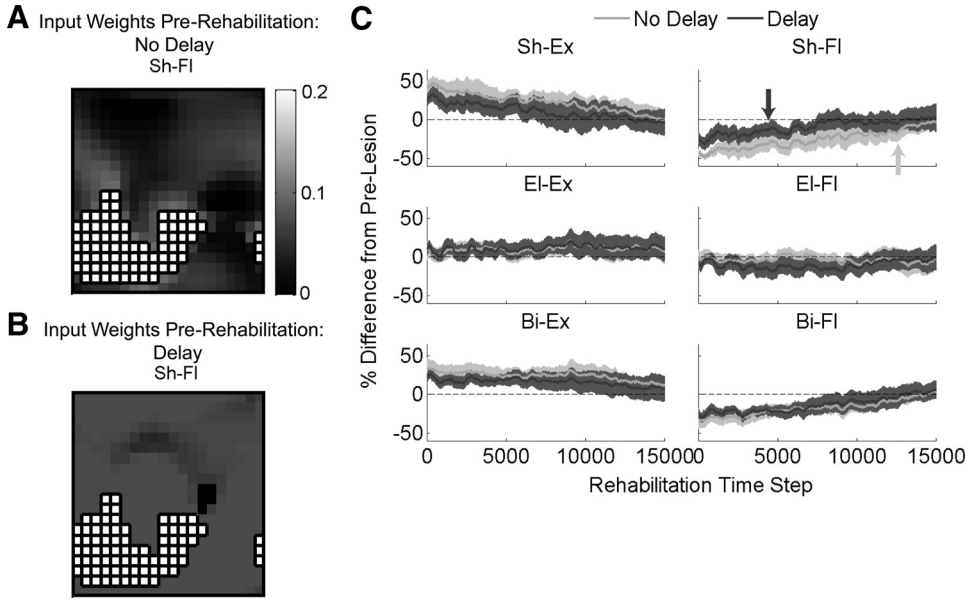

Fig. 5. Delay vs. No Delay Hebbian/homeoplastic rehabilitation. *A* and *B*: input weight maps for lesion-targeted Sh-Fl spindle at beginning of rehabilitation dose in No Delay condition (i.e., immediately after lesion) and Delay condition (i.e., after the delay period), respectively. Note in Delay condition, weights from Sh-Fl spindle have slightly reemerged and become more evenly distributed across network by start of rehabilitation. *C*: percent difference from prelesion of each spindle's input weight proportion during rehabilitation. 0% denotes recovery of the prelesion proportion. For lesion-targeted Sh-Fl spindle, recovery occurs faster in Delay condition (recovery points shown by arrows; based on Wilcoxon signed rank test using a significance level of $P < 0.05$). Shaded error represents mean ± SD.

Parameter Sensitivity Analyses

We ran parameter sensitivity analyses for the delay length, Hebbian learning rate, and homeoplastic learning rate. The mean time courses of Sh-Fl recovery for all altered parameter values are shown in Fig. 7. To test different delays, the same number of time steps of rehabilitation were applied to the network after varying delay lengths. As shown in Fig. 7*A*, recovery during rehabilitation training was slowest with no (0%) delay, as in our main results. This confirmed that the benefits of delay were not dependent on the precise delay length, perhaps excluding delay lengths much shorter than those shown in Fig. 7*A*.

Figure 7, *B* and *C*, shows the recovery results for the Hebbian and homeoplastic learning rates, respectively. Very low learning rates did not achieve recovery within the length of rehabilitation training, while high rates led to unstable recovery, suggesting unstable weight maps that changed drastically based on recent spindle input. High Hebbian learning rates yielded much more frequently changing recovery levels than high homeoplastic learning rates, however.

DISCUSSION

In this simulation study, we explored the influence of cellular Hebbian and homeoplastic mechanisms on recovery poststroke. We notably aimed to answer two important questions regarding neural plasticity mechanisms and rehabilitative therapy in the period poststroke. The first question was whether homeoplasticity was, in addition to Hebbian plasticity, necessary for recovery following a lesion; the second question was whether administering rehabilitation training after a delay period aided recovery.

Regarding the first question, our results clearly showed that recovery in our model was only possible in the presence of both homeoplasticity and Hebbian plasticity. Homeoplasticity abolished local high or low cortical activity patterns seen immediately postlesion. As shown in Fig. 4, this led to very

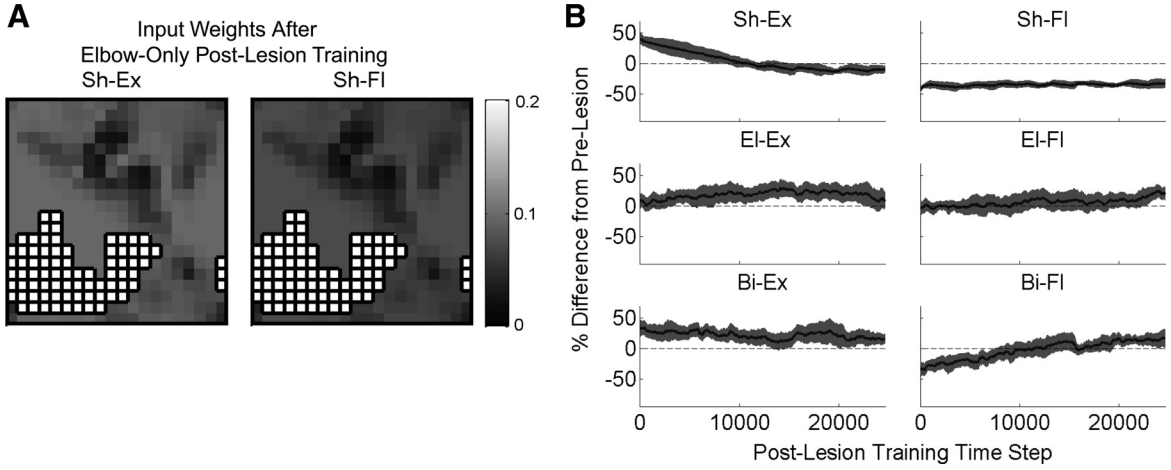

Fig. 6. Elbow-Only postlesion training. *A*: input weight maps for shoulder spindles at end of postlesion training show failure of lesion-targeted Sh-Fl spindle to regain representation and reduced representation of unused Sh-Ex spindle. Compare to Fig. 2*B*. *B*: percent difference from prelesion of each spindle's input weight proportion during postlesion training. 0% Denotes recovery of prelesion proportion. Similar to experimental findings, "nonuse" of affected shoulder in absence of rehabilitation leads to no recovery of affected Sh-Fl spindle, as well as expanded representation beyond prelesion levels in some muscles that were in use during postlesion training (e.g., Bi-Fl). Shaded error represents mean ± SD.

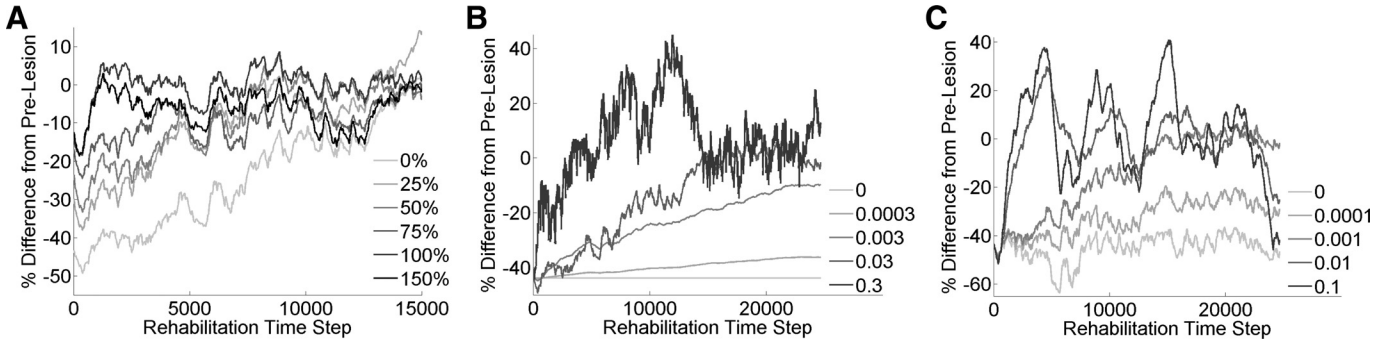

Fig. 7. Parameter sensitivity analyses. Each plot shows mean percent difference from prelesion of targeted Sh-Fl spindle's input weight proportion during rehabilitation. 0% Denotes recovery of prelesion proportion. *A–C*: represent sensitivity analyses for different delays, Hebbian learning rates, and homeoplastic learning rates, respectively. Recovery was robust in all cases except for very low or zero-valued Hebbian or homeoplastic learning rates. Note the *x*-axis of *A* was shortened to clearly show differences in time course for different delays.

different cell membrane potential distributions in the Hebbian/Homeoplastic and Hebbian-Only conditions, which in turn led to different amounts of network reorganization (quantified by cell allegiance changes). In the Hebbian/Homeoplastic condition, the ubiquity of nonzero mean membrane potentials allowed many allegiance changes and thus allowed inputs from the lesion-affected spindle to establish strong connections to the surviving cells. In contrast, in Hebbian-Only networks, local high or low activity patterns were persistent. This, in turn, drove maladaptive plasticity and poor map reorganization by causing many mean cell membrane potentials to remain close to zero, thus preventing reemergence of strong weights from the lesion-targeted Sh-Fl spindle. Parameter sensitivity analyses revealed that it was the presence of both Hebbian and homeoplasticity that was important, not the precise values of their learning rates, since poor recovery only occurred with extreme changes in these learning rates. Note that our explanation of the role of homeoplasticity poststroke is different from, but not mutually exclusive with, previous suggestions that a homeoplastic response to the low levels of perilesional activity immediately postlesion leads to the hyperexcitability seen in the days after lesion (Murphy and Corbett 2009; Nahmani and Turrigiano 2014).

Interestingly, another simulation study reached a similar conclusion on the complementary roles of homeoplasticity and Hebbian plasticity but during visual cortical development (Toyoizumi and Miller 2009). Homeoplasticity was a necessary addition to Hebbian plasticity to allow robust equalization in the representation of both eyes in normal development and overrepresentation of one eye in monocular deprivation. Similar to the present model, homeoplasticity allowed strengthening of initially weak input weights, permitting them to compete effectively for cortical representation against other inputs. Note that in the Toyoizumi and Miller model, very noisy cell activity could compensate for a lack of homeoplasticity (a possibility not explored here); however, compensation was not robust to parameter changes.

Regarding the second question, we found that although recovery and the alleviation of maladaptive plasticity was possible under both No Delay and Delay conditions, a delay led to faster recovery during a subsequent rehabilitation dose. In the Delay condition, during the delay, homeoplasticity led to a "flattening" of input weight distributions; that is, the spindle input weights to each cortical cell became more evenly distributed across all spindles. This was quantified by the overall decrease after delay of the standard deviations of spindle weight values arriving at each cell. This allowed reemergence of weights from the lesion-affected spindles by the beginning of rehabilitation training (Fig. 5), acting as a seed upon which further strengthening and reorganization of lesion-affected spindle weights occurred quickly. In contrast, in the No Delay condition, more time during training was required to achieve any initial weight reemergence. In a link with *experiment 1*, homeoplasticity was required for Sh-Fl reemergence during the delay. This spontaneous reorganization depended on the same effects of homeoplasticity on persistent high or low cortical activity explored in *experiment 1*.

This homeoplastic-dependent mechanism of weight flattening may partially explain (along with activity-induced cell death) poor outcomes seen in rodents and humans when exposed to rehabilitation very early after stroke (Bland et al. 2000; Humm et al. 1999; Kozlowski et al. 1996; Risedal et al. 1999). Note that although the model predicts the same level of recovery after extensive training in both the Delay and No Delay condition, faster recovery in the Delay condition suggests that a limited dose produces better recovery in a short time if given after a delay. Whether this phenomenon occurs biologically could be tested experimentally in rodents by using different rehabilitation dose lengths and different delays before rehabilitation onset to see if for short doses, some delay is beneficial to recovery. This is important clinically because the majority of stroke patients receive only a limited dose of physical therapy that may be insufficient to maximize recovery (Lang et al. 2009).

Further experimental work could also attempt to reduce the ability of peri-infarct cells to undergo homeoplastic adjustments to test our prediction that homeoplasticity is necessary for recovery. However, homeoplasticity in vivo is controlled through a variety of signaling pathways, some of which overlap with LTP pathways (Guzman-Karlsson et al. 2014; Turrigiano 2012; Turrigiano 2011). To minimize overlap, targets for reducing homeoplasticity might be found at the ends of these pathways at the gene transcription or protein trafficking level. For example, genes or promoter sequences for homeostatic processes, such as Na^+ 1β or K^+ K_v1.4 channel subunits (McClung and Nestler 2003) affecting excitability, could be turned off after lesion with optogenetically controlled transcriptional repressors.

Previous experimental work in poststroke monkeys (Nudo et al. 1996) provided a useful benchmark against which to test the capability of our model to reproduce basic biological outcomes. In that work, lesion-targeted inputs only regained

cortical representation if their use was forced during rehabilitation. If they remained unused, they failed to regain representation while allowing other, unlesioned inputs to gain further representation. Here, *experiment 3* showed similar results: simulated disuse of the shoulder after lesioning cells with strong Sh-Fl input prevented recovery of prelesion representation of the Sh-Fl input (Fig. 6). This occurred because relative Sh-Fl spindle inactivity failed to provide the presynaptic activity necessary to increase its input weights via Hebbian plasticity (see *Eq. 3*). This led to the inactive spindles having reduced input weight relative to active spindles, which, because of competitive Hebbian plasticity, increased the active spindles' overall representation beyond prelesion levels.

Limitations and Future Work

Computer simulations of motor recovery poststroke have several benefits when pursued in concert with experimental studies. Simulation allows rapid iteration of theoretical experiments that is not possible biologically. Although simulation results do not amount to proof, they do provide predictions to be developed into hypotheses for testing in vivo. However, the simplifications inherent in simulations necessarily impose a number of limitations on our results.

First, although we proposed here that homeoplasticity (modeled as adjustment of cell excitability) is an important factor in recovery, there are a number of other processes occurring after stroke, including changes in cell signaling and gene regulation prompted by cell death (reviewed in Murphy and Corbett 2009). Experiments that induce lesions with reduced cell death, and hence without some of these secondary lesion effects, could be undertaken by using local cortical cooling (Orton et al. 2012) or blockade of glutamatergic signaling through drug injection (Malmierca et al. 2003).

Second, our model contains highly simplified neuron models. However, we do not expect large changes in results with more complex spiking neurons, because homeoplasticity works over long time scales that filter out individual spikes.

Third, the lack of closed-loop control of the simulated arm meant there was no degradation in arm control after the stroke and no need to produce compensatory actions to achieve reaching goals. Interaction between compensatory behavior and plastic mechanisms presumably further impairs recovery by reinforcing abnormal motor control and will need to be addressed in future models.

While our model is a model of sensory cortex recovery poststroke, recent related modeling studies have explored reorganization in the motor system poststroke. Reorganization of motor system poststroke, unlike purely "unsupervised" sensory system reorganization, requires learning rules that depend on feedback from the environment. In Han et al. (2008), reorganization depends on both error-based, or supervised, and unsupervised learning rules. In an article based on this work, Reinkensmeyer et al. (2012) proposed that reorganization of motor cortical activity to relearn how to flex a simulated wrist depends on reinforcement learning.

Future models of reorganization of the motor system poststroke should aim at better understanding the combined roles of different plastic processes in stroke reorganization. Importantly, they should study how the role of homeoplasticity proposed here interacts with feedback-driven plastic rules in the motor system (Takiyama and Okada 2012). In addition, future models could incorporate interhemispheric effects of lesions (Levitan and Reggia 1999; Reggia 2004) and better link to anatomy. For instance, they could draw on previous work using connectome data to model brain regions as graphical network nodes and evaluating the effects of node deletion on network dynamics (Alstott et al. 2009; Honey and Sporns 2008; Rubinov et al. 2009).

Finally, a crucial aspect of plasticity that is not included in the current model is that various forms of plasticity, such as dendritic and axonal sprouting and LTP, are modulated as a function of time after stroke (i.e., metaplasticity). Following stroke, specific features of brain function revert to those seen at an early stage of development, with the subsequent process of "recovery recapitulating ontogeny" (Cramer and Chopp 2000). In particular, genetic changes in the perilesional area allow for a window of increased plasticity that makes it easier for perilesional neurons to modify existing connections and form new ones in response to motor training (see Murphy and Corbett 2009 for review). Sensorimotor training during this window can drive plasticity more effectively, which benefits recovery if the training involves appropriate rehabilitative movements. On the assumption that rehabilitative training is given before this increased plasticity subsides, our model predicts that a limited dose of training produces better recovery if given after a delay. This prediction, combined with better characterization of the poststroke plasticity window, has important clinical implications for optimally timing the limited dose of physical therapy received by most patients.

APPENDIX

To better characterize the network inputs and understand the pattern of input weights seen after training, the correlations between spindle activities were calculated. Spearman's rank correlation coefficient was used because this measure is nonparametric and does not require the relationship between variables to be linear, only monotonic. The resulting correlation matrix is shown in Fig. A1.

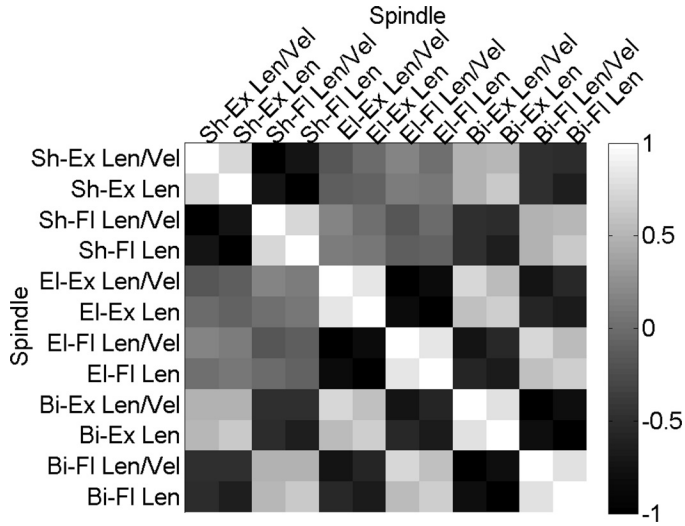

Fig. A1. Correlations in spindle activities during training/rehabilitation dose. Correlations and anticorrelations seen between spindles gave rise to patterns of overlapping or nonoverlapping cortical areas, respectively, of high input weight from certain subsets of spindles seen at end of training.

ACKNOWLEDGMENTS

A. S. Bains thanks Yukikazu Hidaka for useful discussions and advice on the design of the neural network.

GRANTS

A. S. Bains acknowledges the National Sceince Foundation Graduate Research Fellowship and N. Schweighofer acknowledges National Heart, Lung, and Blood Institute Grant R01-HD-065438 for support.

DISCLOSURES

No conflicts of interest, financial or otherwise, are declared by the author(s).

AUTHOR CONTRIBUTIONS

Author contributions: A.S.B. and N.S. conception and design of research; A.S.B. performed experiments; A.S.B. analyzed data; A.S.B. and N.S. interpreted results of experiments; A.S.B. prepared figures; A.S.B. drafted manuscript; A.S.B. and N.S. edited and revised manuscript; N.S. approved final version of manuscript.

REFERENCES

Alstott J, Breakspear M, Hagmann P, Cammoun L, Sporns O. Modeling the impact of lesions in the human brain. *PLoS Comput Biol* 5: e1000408, 2009.

Arbib MA. *The Handbook of Brain Theory and Neural Networks*. Cambridge, MA: MIT Press, 1995, p. xv.

Biernaskie J, Chernenko G, Corbett D. Efficacy of rehabilitative experience declines with time after focal ischemic brain injury. *J Neurosci* 24: 1245–1254, 2004.

Bland ST, Schallert T, Strong R, Aronowski J, Grotta JC, Feeney DM. Early exclusive use of the affected forelimb after moderate transient focal ischemia in rats: functional and anatomic outcome. *Stroke* 31: 1144–1152, 2000.

Boucsein C, Nawrot MP, Schnepel P, Aertsen A. Beyond the cortical column: abundance and physiology of horizontal connections imply a strong role for inputs from the surround. *Front Neurosci* 5: 32, 2011.

Brown CE, Aminoltejari K, Erb H, Winship IR, Murphy TH. In vivo voltage-sensitive dye imaging in adult mice reveals that somatosensory maps lost to stroke are replaced over weeks by new structural and functional circuits with prolonged modes of activation within both the peri-infarct zone and distant sites. *J Neurosci* 29: 1719–1734, 2009.

Buchkremer-Ratzmann I, Witte OW. Extended brain disinhibition following small photothrombotic lesions in rat frontal cortex. *Neuroreport* 8: 519–522, 1997.

Butefisch CM, Netz J, Wessling M, Seitz RJ, Homberg V. Remote changes in cortical excitability after stroke. *Brain* 126: 470–481, 2003.

Butko NJ, Triesch J. Exploring the role of intrinsic plasticity for the learning of sensory representations. In: *European Symposium on Artificial Neural Networks*. Bruges, Belgium: ESANN, 2006.

Castillo PE, Chiu CQ, Carroll RC. Long-term plasticity at inhibitory synapses. *Curr Opin Neurobiol* 21: 328–338, 2011.

Citri A, Malenka RC. Synaptic plasticity: multiple forms, functions, mechanisms. *Neuropsychopharmacology* 33: 18–41, 2008.

Clarkson AN, Huang BS, Macisaac SE, Mody I, Carmichael ST. Reducing excessive GABA-mediated tonic inhibition promotes functional recovery after stroke. *Nature* 468: 305–309, 2010.

Cramer SC, Chopp M. Recovery recapitulates ontogeny. *Trends Neurosci* 23: 265–271, 2000.

Derdikman D, Hildesheim R, Ahissar E, Arieli A, Grinvald A. Imaging spatiotemporal dynamics of surround inhibition in the barrels somatosensory cortex. *J Neurosci* 23: 3100–3105, 2003.

Desai NS, Nelson SB, Turrigiano GG. Activity-dependent regulation of excitability in rat visual cortical neurons. *Neurocomputing* 26–27: 101–106, 1999.

Dromerick AW, Lang CE, Birkenmeier RL, Wagner JM, Miller JP, Videen TO, Powers WJ, Wolf SL, Edwards DF. Very early constraint-induced movement during stroke rehabilitation (VECTORS): a single-center RCT. *Neurology* 73: 195–201, 2009.

Flash T, Hogan N. The coordination of arm movements: an experimentally confirmed mathematical model. *J Neurosci* 5: 1688–1703, 1985.

Foldiak P. Forming sparse representations by local anti-Hebbian learning. *Biol Cybern* 64: 165–170, 1990.

Goodall S, Reggia JA, Chen Y, Ruppin E, Whitney C. A computational model of acute focal cortical lesions. *Stroke* 28: 101–109, 1997.

Guzman-Karlsson MC, Meadows JP, Gavin CF, Hablitz JJ, Sweatt JD. Transcriptional and epigenetic regulation of Hebbian and non-Hebbian plasticity. *Neuropharmacology* 80: 3–17, 2014.

Hagemann G, Redecker C, Neumann-Haefelin T, Freund HJ, Witte OW. Increased long-term potentiation in the surround of experimentally induced focal cortical infarction. *Ann Neurol* 44: 255–258, 1998.

Han CE, Arbib MA, Schweighofer N. Stroke rehabilitation reaches a threshold. *PLoS Comput Biol* 4: e1000133, 2008.

Honey CJ, Sporns O. Dynamical consequences of lesions in cortical networks. *Hum Brain Mapp* 29: 802–809, 2008.

Horn SD, DeJong G, Smout RJ, Gassaway J, James R, Conroy B. Stroke rehabilitation patients, practice, and outcomes: is earlier and more aggressive therapy better? *Arch Phys Med Rehabil* 86: S101–S114, 2005.

Humm JL, Kozlowski DA, Bland ST, James DC, Schallert T. Use-dependent exaggeration of brain injury: is glutamate involved? *Exp Neurol* 157: 349–358, 1999.

Jones EG. Cortical and subcortical contributions to activity-dependent plasticity in primate somatosensory cortex. *Annu Revi Neurosci* 23: 1–37, 2000.

Katayama M, Kawato M. Virtual trajectory and stiffness ellipse during multijoint arm movement predicted by neural inverse models. *Biol Cybern* 69: 353–362, 1993.

Kleim JA, Barbay S, Nudo RJ. Functional reorganization of the rat motor cortex following motor skill learning. *J Neurophysiol* 80: 3321–3325, 1998.

Kleim JA, Bruneau R, VandenBerg P, MacDonald E, Mulrooney R, Pocock D. Motor cortex stimulation enhances motor recovery and reduces peri-infarct dysfunction following ischemic insult. *Neurol Res* 25: 789–793, 2003.

Kohonen T. Self-organized formation of topologically correct feature maps. *Biol Cybern* 43: 59–69, 1982.

Kozlowski DA, James DC, Schallert T. Use-dependent exaggeration of neuronal injury after unilateral sensorimotor cortex lesions. *J Neurosci* 16: 4776–4786, 1996.

Lang CE, Macdonald JR, Reisman DS, Boyd L, Jacobson Kimberley T, Schindler-Ivens SM, Hornby TG, Ross SA, Scheets PL. Observation of amounts of movement practice provided during stroke rehabilitation. *Arch Phys Med Rehabil* 90: 1692–1698, 2009.

LeMasson G, Marder E, Abbott LF. Activity-dependent regulation of conductances in model neurons. *Science* 259: 1915–1917, 1993.

Levitan S, Reggia JA. Interhemispheric effects on map organization following simulated cortical lesions. *Artif Intell Med* 17: 59–85, 1999.

Liepert J, Storch P, Fritsch A, Weiller C. Motor cortex disinhibition in acute stroke. *Clin Neurophysiol* 111: 671–676, 2000.

Linsker R. How to generate ordered maps by maximizing the mutual information between input and output signals. *Neural Comput* 1: 402–411, 1989.

Lytton WW, Stark JM, Yamasaki DS, Sober SJ. Review: computer models of stroke recovery: implications for neurorehabilitation. *Neuroscientist* 5: 100–111, 1999.

MacKenzie IS. A note on the information-theoretic basis of Fitts' law. *J Mot Behav* 21: 323–330, 1989.

Madison DV, Malenka RC, Nicoll RA. Mechanisms underlying long-term potentiation of synaptic transmission. *Annu Rev Neurosci* 14: 379–397, 1991.

Malmierca MS, Hernandez O, Falconi A, Lopez-Poveda EA, Merchan M, Rees A. The commissure of the inferior colliculus shapes frequency response areas in rat: an in vivo study using reversible blockade with microinjection of kynurenic acid. *Exp Brain Res* 153: 522–529, 2003.

Malsburg CV. Self-organization of orientation sensitive cells in striate cortex. *Kybernetik* 14: 85–100, 1973.

Maulden SA, Gassaway J, Horn SD, Smout RJ, DeJong G. Timing of initiation of rehabilitation after stroke. *Arch Phys Med Rehabil* 86: S34–S40, 2005.

McClung CA, Nestler EJ. Regulation of gene expression and cocaine reward by CREB and DeltaFosB. *Nat Neurosci* 6: 1208–1215, 2003.

Mittmann T, Qu M, Zilles K, Luhmann HJ. Long-term cellular dysfunction after focal cerebral ischemia: in vitro analyses. *Neuroscience* 85: 15–27, 1998.

Murphy TH, Corbett D. Plasticity during stroke recovery: from synapse to behaviour. *Nat Rev Neurosci* 10: 861–872, 2009.

Nahmani M, Turrigiano GG. Adult cortical plasticity following injury: recapitulation of critical period mechanisms? *Neuroscience* pii: S0306–4522(14)00331–5, 2014.

Nudo RJ, Milliken GW. Reorganization of movement representations in primary motor cortex following focal ischemic infarcts in adult squirrel monkeys. *J Neurophysiol* 75: 2144–2149, 1996.

Nudo RJ, Wise BM, SiFuentes F, Milliken GW. Neural substrates for the effects of rehabilitative training on motor recovery after ischemic infarct. *Science* 272: 1791–1794, 1996.

Orton LD, Poon PW, Rees A. Deactivation of the inferior colliculus by cooling demonstrates intercollicular modulation of neuronal activity. *Front Neural Circ* 6: 100, 2012.

Plautz EJ, Milliken GW, Nudo RJ. Effects of repetitive motor training on movement representations in adult squirrel monkeys: role of use versus learning. *Neurobiol Learn Mem* 74: 27–55, 2000.

Qu M, Mittmann T, Luhmann HJ, Schleicher A, Zilles K. Long-term changes of ionotropic glutamate and GABA receptors after unilateral permanent focal cerebral ischemia in the mouse brain. *Neuroscience* 85: 29–43, 1998.

Reggia JA. Neurocomputational models of the remote effects of focal brain damage. *Med Eng Phys* 26: 711–722, 2004.

Reinkensmeyer DJ, Guigon E, Maier MA. A computational model of use-dependent motor recovery following a stroke: optimizing corticospinal activations via reinforcement learning can explain residual capacity and other strength recovery dynamics. *Neural Netw* 29–30: 60–69, 2012.

Risedal A, Zeng J, Johansson BB. Early training may exacerbate brain damage after focal brain ischemia in the rat. *J Cereb Blood Flow Metab* 19: 997–1003, 1999.

Rubinov M, McIntosh AR, Valenzuela MJ, Breakspear M. Simulation of neuronal death and network recovery in a computational model of distributed cortical activity. *Am J Geriatr Psychiatry* 17: 210–217, 2009.

Salter K, Jutai J, Hartley M, Foley N, Bhogal S, Bayona N, Teasell R. Impact of early vs. delayed admission to rehabilitation on functional outcomes in persons with stroke. *J Rehab Med* 38: 113–117, 2006.

Sanes JN, Donoghue JP. Plasticity and primary motor cortex. *Annu Rev Neurosci* 23: 393–415, 2000.

Schiene K, Bruehl C, Zilles K, Qü M, Hagemann G, Kraemer M, Witte OW. Neuronal hyperexcitability and reduction of GABAA-receptor expression in the surround of cerebral photothrombosis. *J Cereb Blood Flow Metab* 16: 906–914, 1996.

Sigler A, Mohajerani MH, Murphy TH. Imaging rapid redistribution of sensory-evoked depolarization through existing cortical pathways after targeted stroke in mice. *Proc Natl Acad Sci USA* 106: 11759–11764, 2009.

Sirosh J, Miikkulainen R. Topographic receptive fields and patterned lateral interaction in a self-organizing model of the primary visual cortex. *Neural Comput* 9: 577–594, 1997.

Sober SJ, Stark JM, Yamasaki DS, Lytton WW. Receptive field changes after strokelike cortical ablation: a role for activation dynamics. *J Neurophysiol* 78: 3438–3443, 1997.

Stepanyants A, Martinez LM, Ferecsko AS, Kisvarday ZF. The fractions of short- and long-range connections in the visual cortex. *Proc Natl Acad Sci USA* 106: 3555–3560, 2009.

Stevens JL, Law JS, Antolik J, Bednar JA. Mechanisms for stable, robust, and adaptive development of orientation maps in the primary visual cortex. *J Neurosci* 33: 15747–15766, 2013.

Sullivan TJ, de Sa VR. Homeostatic synaptic scaling in self-organizing maps. *Neural Netw* 19: 734–743, 2006.

Takiyama K, Okada M. Recovery in stroke rehabilitation through the rotation of preferred directions induced by bimanual movements: a computational study. *PLoS One* 7: e37594, 2012.

Toyoizumi T, Miller KD. Equalization of ocular dominance columns induced by an activity-dependent learning rule and the maturation of inhibition. *J Neurosci* 29: 6514–6525, 2009.

Triesch J. A gradient rule for the plasticity of a neuron's intrinsic excitability. *Proc Intl Conf Artif Neural Netw*, 2005, p. 1–7.

Turrigiano G. Homeostatic synaptic plasticity: local and global mechanisms for stabilizing neuronal function. *Cold Spring Harb Perspect Biol* 4: a005736, 2012.

Turrigiano G. Too many cooks? Intrinsic and synaptic homeostatic mechanisms in cortical circuit refinement. *Annu Rev Neurosci* 34: 89–103, 2011.

Wilson SP, Law JS, Mitchinson B, Prescott TJ, Bednar JA. Modeling the emergence of whisker direction maps in rat barrel cortex. *PLoS One* 5: e8778, 2010.

Winship IR, Murphy TH. Remapping the somatosensory cortex after stroke: insight from imaging the synapse to network. *Neuroscientist* 15: 507–524, 2009.

Wolf SL, Thompson PA, Winstein CJ, Miller JP, Blanton SR, Nichols-Larsen DS, Morris DM, Uswatte G, Taub E, Light KE, Sawaki L. The EXCITE stroke trial: comparing early and delayed constraint-induced movement therapy. *Stroke* 41: 2309–2315, 2010.

Wolf SL, Winstein CJ, Miller JP, Taub E, Uswatte G, Morris D, Giuliani C, Light KE, Nichols-Larsen D. Effect of constraint-induced movement therapy on upper extremity function 3 to 9 months after stroke: the EXCITE randomized clinical trial. *JAMA* 296: 2095–2104, 2006.